SEISMIC DESIGN ANALYSIS OF A SHALLOW-BURIED SUBWAY STATION IN LIQUEFIABLE SOILS

E. Zhai[1] and B. O'Neill[2]

[1] *Principal Engineer, Kleinfelder West, Inc., Irvine, California, USA*
[2] *Principal Engineer, Kleinfelder West, Inc., Oakland, California, USA*
Email: ezhai@kleinfelder.com, boneill@kleinfelder.com

ABSTRACT :

During the recent design of a 16.3-mile (26.2-km) long rapid transit project which extends the Bay Area Rapid Transit system into Santa Clara Valley and San Jose areas in northern California, shallow-buried (cut-and-cover) box structures were proposed for the subway stations. The Downtown San Jose Station is located in alluvial soils including layers of saturated sand with corrected SPT N-value of 14 to 27, indicating high potential of liquefaction subject to the design earthquake. To characterize the site, a field exploration program was performed which consisted of cone penetration test soundings and drilled borings with standard penetration tests. Laboratory tests were assigned on selected soil samples to develop soil properties including cyclic triaxial testing to determine the cyclic strength of the layers susceptible to liquefaction. This paper focused on geotechnical hazards and seismic design methods, geotechnical design parameters, a practical-oriented pore pressure generation model, and seismic time-history design analyses of the subway structure. The analysis results indicated that the ratio of the maximum seismic racking deformation versus the height of the box structure is approximately 1 percent, which compares to about 0.4 percent if liquefaction would not occur. It was recommended that such a large racking deformation due to liquefaction should be designed with adequate structural ductility and strength; rather than more expensive ground improvements in the Downtown area.

KEYWORDS: Seismic Design, Subway Station, Cut-and-Cover, Liquefaction, SSI Analysis, FLAC

1. INTRODUCTION

The Bay Area Rapid Transit system will include a 16.3-mile (26.2-km) long extension to Santa Clara Valley and San Jose areas which is under design at a 65 percent completion. The design consisted of at-grade, depressed 'trench' (U-shaped Walls) segments, and tunnel segments. Three shallow-buried box structures were proposed for the subway stations in San Jose area using cut-and-cover construction methods. Temporary dewatering, excavation and shoring will be required for constructing the subway stations. A continuous deep soil mixing (DSM) wall was proposed to provide temporary shoring and also to serve as a groundwater cut-off wall. This wall system is under further review and an alternative is to use slurry wall due to required groundwater cut-off up to 175 feet deep. This alternative has not been considered in the preliminary (35 percent completion) and the current design phases. The current design criteria require that the stiffness of the DSM shoring be ignored for seismic design of the permanent station box structure. The subway stations will be interconnected by twin tunnels constructed using closed-face tunnel boring machine (TBM) methods. This paper presents our seismic design approach and results for Downtown San Jose Station to be buried in liquefiable soils. Geotechnical field investigation and laboratory testing were performed to characterize the site subsurface conditions, and to determine the cyclic strength and post-liquefaction residual strength of the liquefiable layers. Key geotechnical hazards at the project site were identified to include high seismic shaking and liquefaction. Mitigation measures such as ground improvements were evaluated, but considered not economical due to possible interference with heavy traffic and dense underground utilities. It was decided that ductile structural components be designed and constructed to withstand seismic racking. A nonlinear effective-stress time-history soil-structure-interaction (SSI) design analysis approach was used to evaluate the seismic demands. Design analyses started with static SSI analyses to consider dewatering, installation of soil cement/soldier pile wall, staged excavations and placement of box structure, followed by nonlinear dynamic time history analyses. Six input (3 sets) acceleration time histories were developed which had compatible response spectra as required. The analysis results included racking deformations, joint rotations, shear forces and bending moments. Static and dynamic soil pressures were also provided.

2. DEVELOPMENT OF DESIGN GROUND MOTIONS

Seismic hazard evaluation was performed using both deterministic and probabilistic methods. Seismic design criteria for this project requires that the higher ground motions from a site-specific 10% in 50 year probabilistic seismic hazard analysis or the median plus 0.5 standard deviation of ground motions from a deterministic seismic hazard analysis based on the nearby controlling faults of San Andreas fault (Mw 8.0), Hayward fault (Mw 7.25) and Calaveras fault (Mw 7.0) should be used in the design. Time history analyses were performed using a minimum of three sets of spectrum compatible time histories. Each set contains fault-normal, fault parallel and vertical ground motion time histories. The largest displacement obtained from the three sets of time histories should be used for design. Seed acceleration time histories were selected from the recordings at Coyote Lake from the 1989 Loma Prieta earthquake, Nishi-Akashi from the 1995 Kobe earthquake, and Izmit from the 1999 Kocaeli earthquake, based on the geological and seismological conditions of the site. These seed time histories were spectrally-matched to the design target response spectra as outcropping motions for a Type C soil condition which roughly corresponds to soils at a 400 feet (122 m) depth. We used the computer program SHAKE to deconvolve these outcropping motions to depth 400 feet (122 m) and further computed the response motions at the depth of SSI model base at a depth of 250 feet (76.2 m). Figure 1 presents the fault-normal (FN) and fault-parallel (FP) components of the deconvoluted input motions at the SSI model base at a depth of 250 feet (76.2 m).

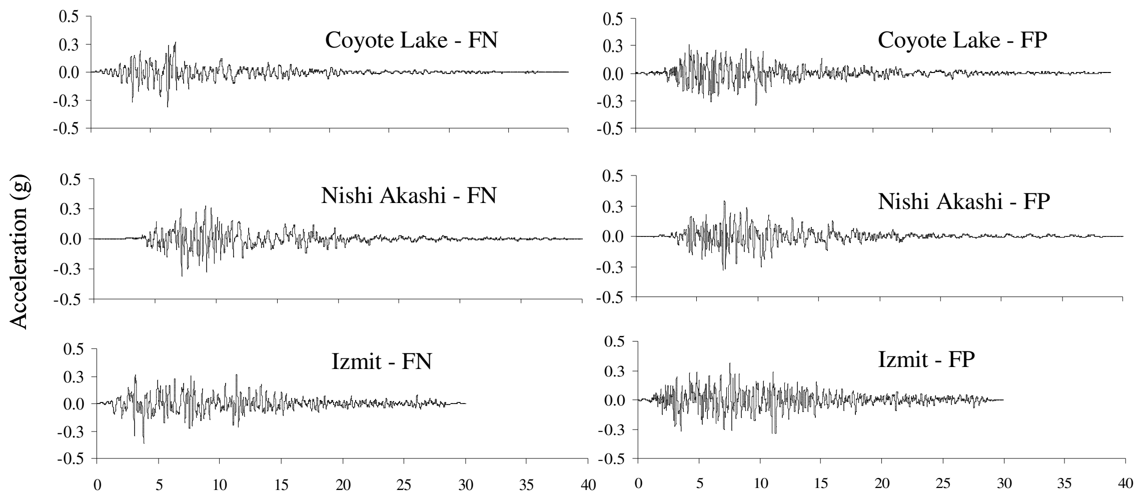

Figure 1 Deconvoluted input motions at FLAC model base

3. FLAC SSI MODEL AND MATERIAL PROPERTIES

3.1 Model Makeup

Structural components and their physical properties of the proposed tunnel stations are listed in Table 1. All structural components were modeled as 2-dimensional beam elements with the commercial computer program FLAC (Itasca, 2005). The slabs are assumed to perform elastically during the design earthquake and the walls and columns are to be designed as ductile components. Plastic moments listed in the table were assigned in the dynamic SSI analysis. All input properties and output forces and moments are per foot (0.3 m) of the walls and slabs, and per column of the upper and lower columns. Structural roof and invert slabs interact with soil grids by connecting the structural nodes with the soil grid points. The walls interact with soils using the interface elements. Soil properties were derived based on a field exploration program, which included soil borings and cone penetration test (CPT) soundings, and the laboratory testing results. Table 2 summaries the soil properties used in the SSI analyses. The vertical dimension of the SSI model mesh is from elevation of 88 feet (26.8 m) to

-162 feet (-49.4 m). The horizontal dimension is 300 feet (91.5 m) with the box structure symmetrical to the center in the horizontal direction. In the initial static analysis to compute in-situ stresses, the base boundary was fixed both horizontally and vertically and the side boundaries were only fixed horizontally. In the dynamic analysis, the input motion was applied at the base boundary. The horizontal restraints of the side boundaries were released and replaced with the free-field boundaries. The plane waves propagating upward suffer little distortion at the boundary because the free-field grid supplies conditions that are identical to those in an infinite model.

Table 1 Box structure's geometry and physical properties

No.	Structural Component Name	Plain-Strain View Dimensions (ft)			Unit Weight (pcf)	Moment of Inertia (in^4/ft)		Young's Modulus (ksi)	Plastic Moment if ductility allowed (kip-ft)
		Vertical Dimension	Horizontal Dimension	Bottom Elevation		Full	Cracked		
1	soil cover	8.00	n/a	-8.00	125	n/a	n/a	n/a	n/a
2	roof slab	2.50	60.50	-10.50	150	27000	n/a	3605	n/a
3	left upper wall	18.00	2.00	-28.50	150	13824	2109	3605	122
4	upper column	18.00	3.00	-28.50	150	3999	3165	4031	123
5	right upper wall	18.00	2.00	-28.50	150	13824	2109	3605	122
6	concouse slab	1.00	60.50	-29.50	150	1728	n/a	3605	n/a
7	left lower wall	21.83	2.50	-51.33	150	27000	5980	3605	278
8	lower column	21.83	3.00	-51.33	150	3999	3165	4031	123
9	right lower wall	21.83	2.50	-51.33	150	27000	5980	3605	278
10	bottom slab	5.00	60.50	-56.33	150	216000	n/a	3605	n/a

Table 2 Soil properties

No. of Soil Layer	Elevation[1)] (ft)		USCS Soil Type	Total Unit Weight (pcf)	Total Stress Shear Strength		Equivalent SPT $(N_1)60$	Equivalent (corrected) SPT $(N_1)60_{cs}$ for Sandy layer	Shear Wave Velocity (ft/sec)	Shear Modulus (psf)	Poisson's Ratio	Bulk Modulus (K) (psf)
	From	To			C (psf)	phi (deg)						
1	88	82	SM	118	0	32	12	18	700	1.80E+06	0.25	2.99E+06
2	82	76	SM	118	0	32	12	18	625	1.43E+06	0.25	2.39E+06
3	76	69	CL	120	1000	0	-	-	550	1.13E+06	0.45	1.09E+07
4	69	62	CL	120	1250	0	-	-	700	1.83E+06	0.45	1.77E+07
5	62	55	SM	125	0	34	7 to 25 (avg.14)	14 to 27 (avg. 20)	725	2.04E+06	0.25	3.40E+06
6	55	48	SM	125	0	34	8 to 25 (avg.14)	15 to 27 (avg. 20)	700	1.90E+06	0.25	3.17E+06
7	48	41	CL	125	1500	0	-	-	700	1.90E+06	0.45	1.84E+07
8	41	34	CL	125	1750	0	-	-	725	2.04E+06	0.45	1.97E+07
9	34	27	CL	125	2000	0	-	-	800	2.48E+06	0.45	2.40E+07
10	27	20	CL	125	2250	0	-	-	900	3.14E+06	0.45	3.04E+07
11	20	13	CL	125	2500	0	-	-	900	3.14E+06	0.45	3.04E+07
12	13	3	SW-SM	135	0	36	30	>30	1000	4.19E+06	0.35	1.26E+07
13	3	-7	SW-SM	135	0	36	30	>30	1000	4.19E+06	0.35	1.26E+07
14	-7	-17	CL	126	3000	0	-	-	1100	4.73E+06	0.45	4.58E+07
15	-17	-27	CL	126	3000	0	-	-	1050	4.31E+06	0.45	4.17E+07
16	-27	-37	SC	128	0	38	50	>50	1100	4.81E+06	0.35	1.44E+07
17	-37	-62	CL	128	4000	0	-	-	1100	4.81E+06	0.45	4.65E+07
18	-62	-87	GC	135	0	40	50	>50	1200	6.04E+06	0.35	1.81E+07
19	-87	-112	GC	135	0	40	50	>50	1200	6.04E+06	0.35	1.81E+07
20	-112	-137	CL	130	4000	0	-	-	1300	6.82E+06	0.45	6.60E+07
21	-137	-162	CL	130	4000	0	-	-	1400	7.91E+06	0.45	7.65E+07

3.2 Nonlinear Effective-Stress Analysis

3.2.1 Analysis Approach

We used a Mohr-Coulomb (linear elastic/perfectly plastic) soil model coupled with a practice-oriented pore-pressure generation model (Dawson et al., 2001, Zhai et al., 2004) which were programmed into FLAC using programming language FISH that is embedded within FLAC. Pore pressures are generated in response to shear stress cycles, as illustrated schematically in Figure 2, which follow the cyclic-stress approach developed by Seed and coworkers (Seed, et al., 1976, 1979). However, unlike the standard approach where liquefaction potential is assessed as a post-processing step, pore-pressure generation in FLAC is incremental and fully integrated with the nonlinear dynamic analysis. As effective stresses decrease with increasing pore water pressure, the soil begins to yield and increments of permanent deformation are accumulated during shaking. The simultaneous coupling of pore-pressure generation with nonlinear, plasticity based, stress analysis produces a more realistic dynamic response. Specifically, the plastic strains generated as a result of increased pore pressures significantly contribute to the internal damping of the modeled earth structure. The analysis approach described above has been verified by analyzing well documented seismic-performance case histories of dams, as well as performing validation analysis of centrifuge shaking test as part of the NSF-sponsored VELACS program (Zhai et al., 2004). It has been utilized in practice for various earth fill dams and for dynamic soil-structure interaction analyses of pile-supported structures (Zhai, et al., 2007).

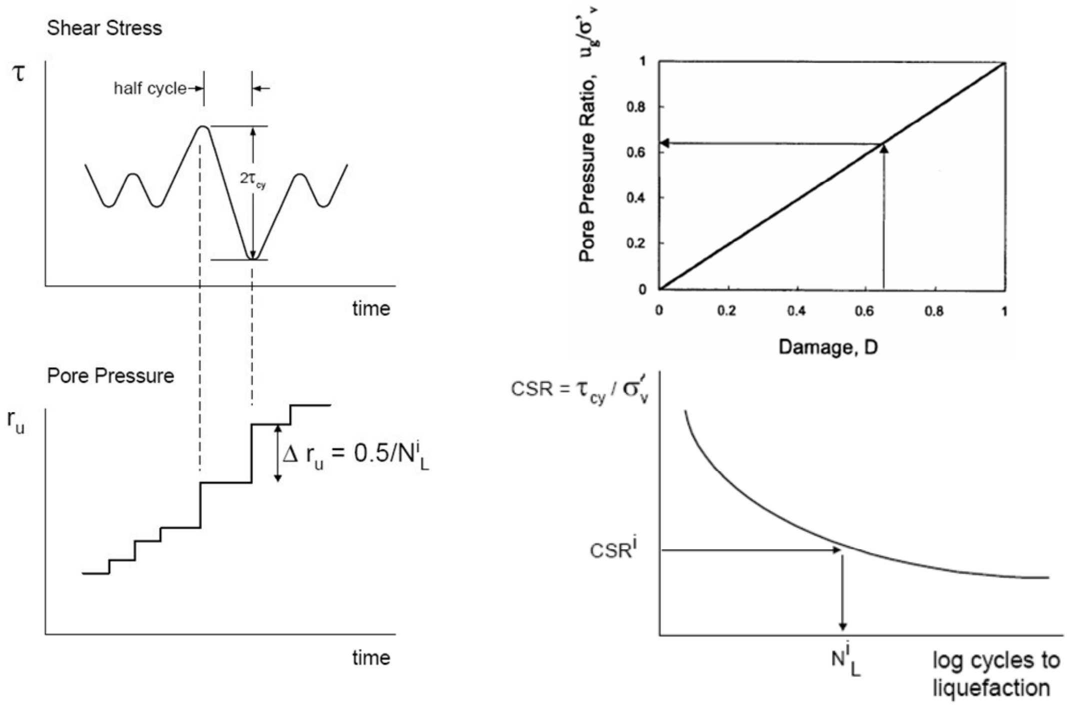

Figure 2 Pore pressure generation scheme (Dawson et al., 2001)

3.2.2 Cyclic Strength Curves

The pore-pressure generation scheme utilized in the nonlinear effective-stress analysis requires as input a cyclic-strength curve, a relation between the cyclic-stress ratio and the number of cycles required to reach liquefaction. Consolidated Undrained Cyclic Triaxial (CUCTX) laboratory testing was performed on samples selected at the depth where liquefaction was identified using the simplified liquefaction analysis procedure recommended by Youd et al. (2001). The sampled were X-Ray'ed after being transported to a remote laboratory for quality control. X-Ray radiography provides a qualitative measure of the internal structure of the sample's content. The testing procedure generally followed ASTM D-4452. Qualified samples were then selected for CUCTX testing which generally followed ASTM D-5311 procedure. The results from the CUCTX testing were plotted in Figure 3. Also plotted in Figure 3 are cyclic strength curves derived from equivalent SPT blow counts $(N_1)60cs$ corrected for clean sand using the empirical relationship by Youd et al. (2001). For our analysis, a lower-bound cyclic strength curve was selected which was further approximated by best-fit straight-lines shown as solid lines in Figure 3. Post-liquefaction residual strengths of liquefiable layers were derived from the mean of the upper bound and lower bound curves (Seed and Harder, 1990).

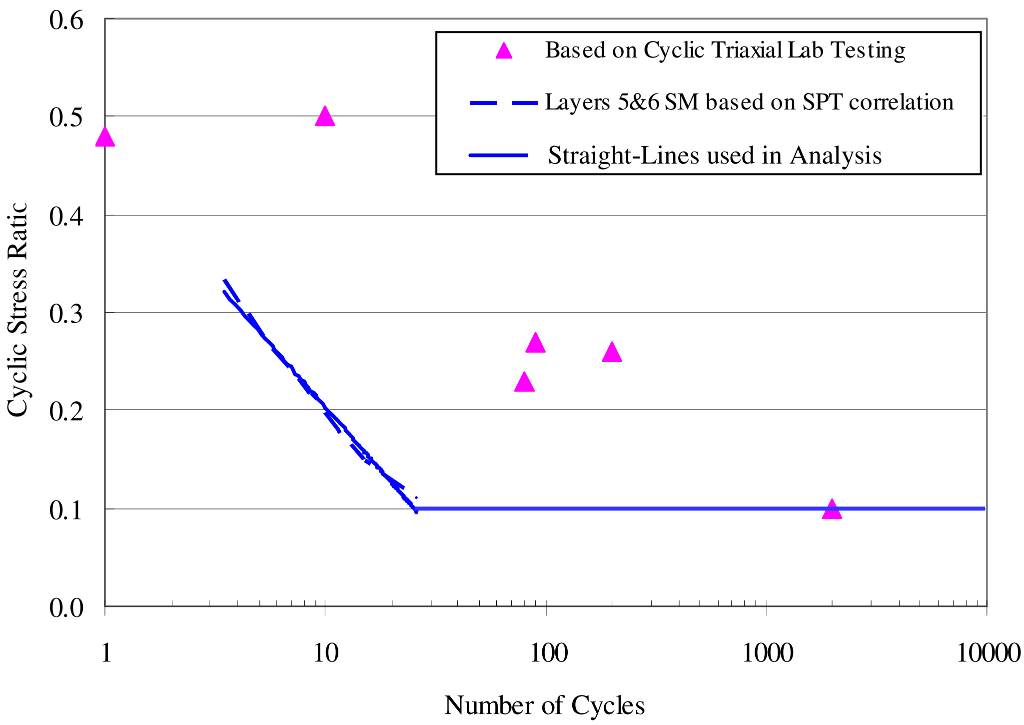

Figure 3 Cyclic shear strength curves of liquefiable layers

3.2.3 Hysteretic Damping

Damping in soils is primarily hysteretic, since energy dissipation occurs when grains slide over one another. In the Mohr-Coulomb law utilized herein, energy is dissipated by shaking-induced plastic flow when shear stresses reach the yield strength. For smaller stress cycles remaining in the elastic range, energy dissipation is achieved by assigning hysteretic damping ratios for each soil grid based on its shear strain arrived at. We used Hardin & Drnevich model (Itasca, FLAC version 5, Optional Features) to develop the input damping coefficient. Strain-compatible shear modulus of each soil layer was computed and updated during shaking following the initial shear modulus as listed in Table 2.

4. NONLINEAR DYNAMIC SSI ANALYSIS

4.1 Free-Field Racking Deformations

Free-field (without box structure) seismic response analyses were performed and repeated for each of the input motions. The results indicated that the 1st input motion Coyote–FN is the controlling input motion that resulted in the maximum racking deformation. The free-field analysis results are plotted in Figure 4. The maximum free-field racking deformation is 3.6 inches. Soil layers between elevations of 62 feet and 48 feet are susceptible for liquefaction subject to the design earthquake.

4.2 SSI Analysis Results

The dynamic SSI analyses were then only performed using the controlling motion Coyote–FN plus the vertical motion. Time history plots of the racking deformations (top slab versus bottom slab), dynamic shear forces at the top and bottom of the sidewall, and dynamic bending moments at the top and bottom of the sidewall are presented in Figure 5. The maximum racking deformation of the box structure is 4.1 inches. The maximum dynamic moment on the wall is 275 kip-ft (negative value) and the maximum dynamic shear on the wall is 19 kips.

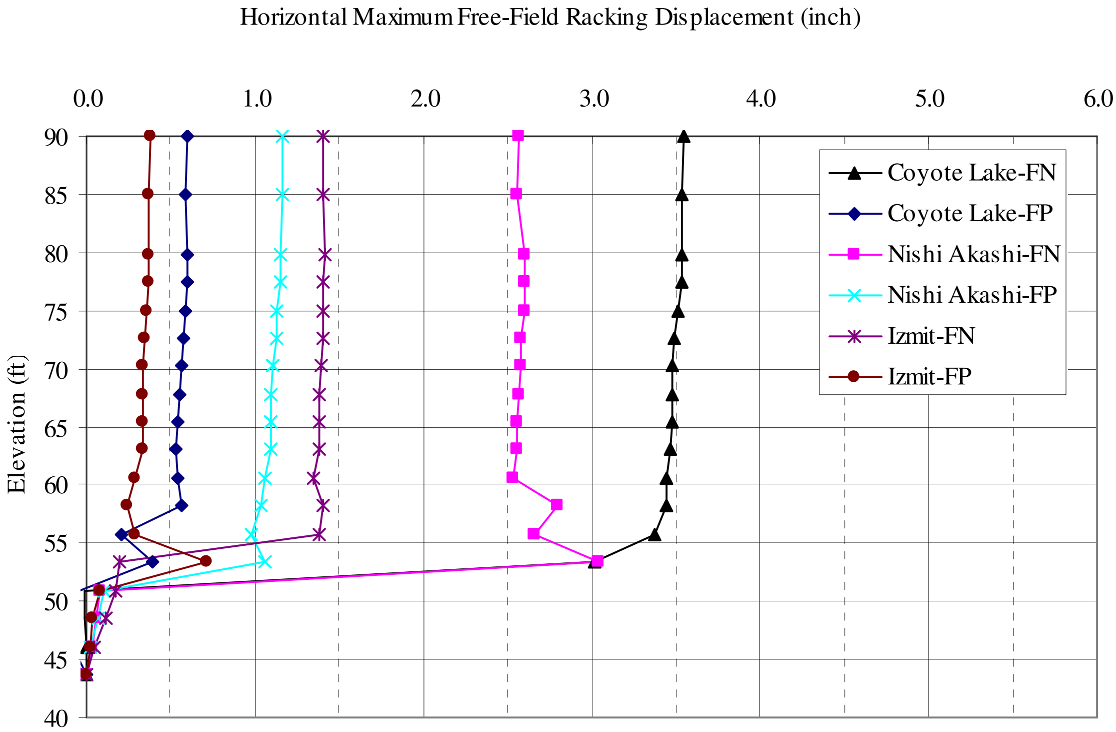

Figure 4 Free-field racking deformations subjected to various input motions

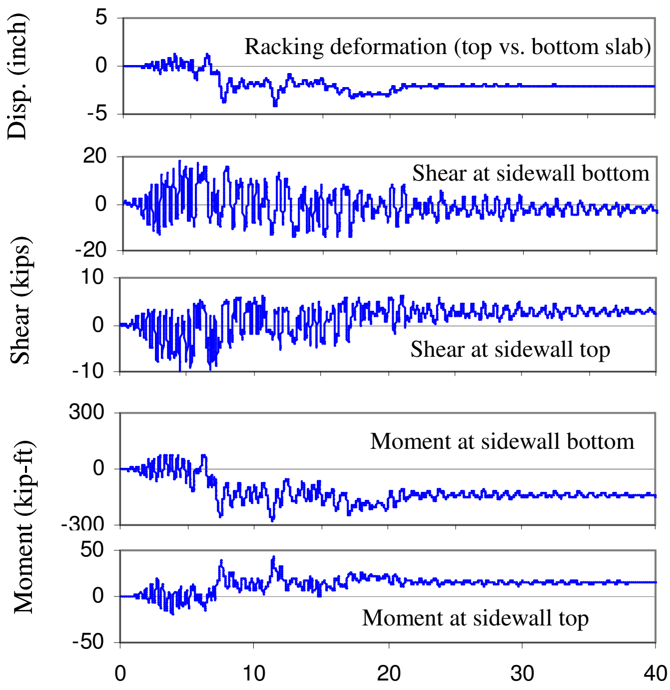

Figure 5 Dynamic SSI Analysis Results

5. CONCLUSIONS

This paper is based on seismic design analyses for the proposed San Jose Downtown Subway Station which is part of a rapid transit system in Northern California, USA. Seismic and geological hazards include strong ground shaking and presence of liquefiable layers on the subway station sidewalls. It was decided to design a ductile structural system to withstand significant racking deformation resulted from seismic shaking and soil liquefaction such that more expensive ground improvement in a densely populated downtown area can be avoided. In order for more realistic design, nonlinear dynamic SSI analysis was selected to compute structural seismic demands.

Our design analysis results indicated that liquefiable layers resulted in a maximum racking deformation of 4.1 inches, indicating that ratio of the maximum seismic racking deformation versus the height of the box structure is approximately 1 percent, which compares to about 0.4 percent if liquefaction would not occur (the analyses were not included in this paper).

We recommend that the subway station structure and appurtenant systems be adequately designed and constructed such that the computed seismic demands are met.

6. ACKNOWLEDGMENT

The work presented in this paper was based on Kleinfelder Project No. 79838. The authors wish to thank Mr. Mark Fuhriman, PE, who provided soil data, and Mr. Edward E. Rinne, PE, GE, who performed QA review for the project. Dr. Liping Yan of Southwest Geotech, Inc. performed QC for some portions of the results.

The authors also thank Mr. Stephen Biggs and Anthony Notaro of Biggs Cardoza Associates, Inc. for their discussions.

REFERENCES

Dawson, E.M. & Roth, W.H. 2001. A practice oriented pore pressure generation model, *2nd FLAC International Symposium*.

Itasca Consulting Group, Inc. 2005. FLAC Version 5, User's manual.

Seed, H.B., Martin, P.P., & Lysmer, J. 1976. Pore-water pressure changes during soil liquefaction, *Journal of the geotechnical engineering division*, ASCE , Vol. 102, No. GT4, pp 323-346.

Seed, H.B. 1979. Soil liquefaction and cyclic mobility evaluation for level ground during earthquakes, *Journal of the geotechnical engineering division*, ASCE, Vol. 105 No. GT2, pp 201-255.

Seed, R. B. &, Harder, L.F. 1990. SPT-based analysis of cyclic pore pressure generation and undrained residual strength, *Proceedings of H.B. Seed memorial symposium*, University of California, Berkeley, Vol. 2, pp. 351-376.

Youd, T.L. & Idriss I.M. 2001. Liquefaction resistance of soils: summary report from the 1996 NCEER and 1998 NCEER/NSF workshops on evaluation of liquefaction resistance of soils, *Journal of the geotechnical and geoenvironmental engineering*, ASCE, Vol. 127, No. 4, pp 297-313.

Zhai, E., K. Bhushan and M. Miyajima, 2004. "Triggering of Liquefaction under Non-Zero Static Driving Shear Stress," *Proceedings of 13th International Conference on Soil Dynamic & Earthquake Engineering & 3rd International Conference on Earthquake Geotechnical Engineering,* Berkeley, Vol.2, pp.589-596.

Zhai, E., K. Bhushan and R. Tognazzi, 2006. "Seismic Design Analysis of CIDH Pile Foundations Subject To Liquefaction-Induced Lateral Spreading & Downdrag." Proceedings of the 8th National Conference on Earthquake Engineering, San Francisco, California.